First-principles calculation of hydrogen vibrations of the H-P complex in silicon

Rolf H. Luchsinger* and Peter F. Meier
Physics Institute, University of Zurich, 8057 Zurich, Switzerland

Yu Zhou
Department of Physics and Minnesota Supercomputer Institute, University of Minnesota, Minneapolis, Minnesota 55455
(Received 30 May 1997)

We present a theoretical investigation of the local vibrational modes of hydrogen in the H-P complex in silicon. The energy surface of the hydrogen is calculated by *ab initio* methods, fitted to a model potential, and the vibrational spectrum is investigated by perturbation theory. A Fermi resonance is found between the second hydrogen-wagging and fundamental stretching modes. The calculated vibrational frequencies compare very well to the experimental results, and confirm a recent assignment of the hydrogen vibrational bands of donor-hydrogen complexes in Si. [S0163-1829(98)05108-X]

I. INTRODUCTION

The behavior of hydrogen in semiconductors has attracted considerable interest in the past few years. This is mainly due to the fact that it can passivate electrically active acceptor and donor impurities by forming neutral complexes.[1,2] Experimental and theoretical studies suggest the following equilibrium configurations for these passivated centers. For an acceptor, H is located close to a bond-center position of one of the Si-acceptor bonds. For a donor, H is on the extension of a Si-donor bond, antibonding to Si. In both cases, the atoms around the H relax accordingly.

The geometry for the passivated donor complex was suggested[3] based on the experimental observation that the vibrational frequencies of H are very low and nearly independent of the donor species. The hydrogen frequencies found at 1555, 1561, and 1562 cm^{-1} for the P, As, and Sb donors,[4] respectively, were attributed to the stretching modes. Two additional bands were observed near 810 and 1660 cm^{-1} for each of the complexes. The 810-cm^{-1} band was assigned to the H-wagging mode, whereas the assignment of the 1660 cm^{-1} band was controversial.[4–7] Recently, Zheng and Stavola[8] proposed an assignment for the vibrational spectra, based upon a Fermi resonance between the second harmonic of the wagging and the fundamental stretching modes. They explained the presence of all three vibrational bands without the need for additional charge states or defect species that have been suggested.[4–7] In addition, they obtained data to confirm their model.

The microscopic electronic structure of H-passivated complexes in semiconductors was the subject of a large number of theoretical investigations. For donor-hydrogen complexes in Si, various techniques were applied, including semiempirical procedures,[9] Hartree-Fock (HF) cluster calculations,[10,11] and methods based on the density-functional (DF) method.[12–16] The results for the equilibrium structure and the vibrational frequencies of the hydrogen generally agree, but some significant discrepancies between HF and DF predictions remain to be explained. HF-like methods in general predict strong bonding between Si and H, with Si-H distances of the order of 1.4 Å and frequencies higher than 2000 cm^{-1} for the axial mode. In contrast, DF-based calculations show a weaker bonding with Si-H distances around 1.6–1.7 Å.[17] The corresponding stretching and wagging modes are lower than the experimental ones.

In the present work, results are reported for the H-P complex in Si, obtained with the DF method in clusters. In Sec. II, the method and the calculated equilibrium geometry are explained. The energy surface of hydrogen is calculated at a very large number of H sties. A model potential which describes this energy surface is discussed in Sec. III. The local vibrational modes of H and D are then determined by solving the Schrödinger equation. As described in Sec. IV, this is done by both a perturbation approach and a numerical solution. Our calculated vibrational spectra support the model by Zheng and Stavola,[8] and provide quantitative results for the anharmonic coupling. Conclusions are in Sec. V.

II. ENERGY SURFACE

In a first step, we determined the equilibrium configuration for hydrogen in P-doped silicon. We started with a cluster consisting of 44 Si atoms and 42 H surface saturators, the positions of which are energy optimized.[2] Next, the innermost pair of atoms was replaced by a Si-P pair, and an additional H was placed between these two atoms. The positions of these three atoms (Si, H, P) as well as those of the six nearest-neighbor Si atoms were then optimized under constraint of C_{3v} symmetry. For these nine atoms, polarization functions were used in addition to the Gaussian double-ζ basis set on all the atoms. Pseudopotentials described the core electrons of Si and P. The calculations were performed with the DF method in the local-density approximation, as implemented in the GAUSSIAN 94 code[18] using the Vosko-Wilk-Nusair local-density functional.[19]

The same optimization procedure was repeated for a H antibonding to P (Si-P-H) and to Si (H-Si-P). In agreement with previous work, the site antibonding to Si was found to be the most stable. The equilibrium configuration is shown in Fig. 1. The positions of the relaxed atoms are close to results from plane-wave DF calculations,[15] which yielded $d_{\text{H-Si}} = 1.618$ Å and $d_{\text{Si-P}} = 2.812$ Å.

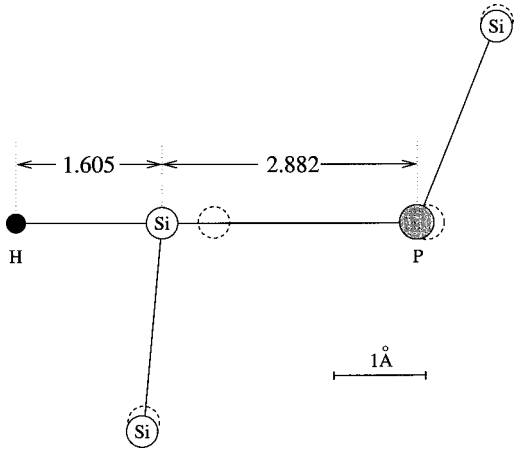

FIG. 1. The calculated equilibrium configuration for H in P-doped Si. The dashed circles indicate unrelaxed positions.

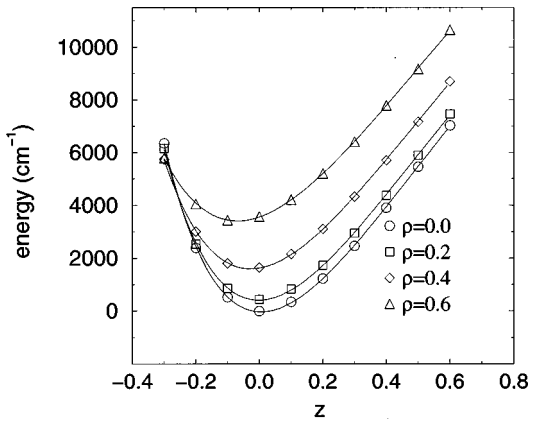

FIG. 2. Energy surface (in cm^{-1}) (Ref. 20) scanned parallel to the symmetry axis. The calculated points are fitted to a Morse potential for each scan. Distances are in Å.

The ⟨111⟩ direction from P to the equilibrium site of H is denoted as the z axis. We explored the energy surface near the equilibrium position z_0. The hydrogen was moved away from its equilibrium site, and the total energy was calculated. The positions of all the other atoms were kept fixed. This assumes that the H or D move much faster than the heavier atoms in the cluster. Only calculations with H along the z axis were feasible in the large cluster. To explore the energies with H away from this axis, where most of the symmetry is lacking, the smaller cluster $Si_{13}HPH_{24}$ was used with the same atomic positions as optimized in the large cluster. The energy variations relative to the equilibrium site are in very good agreement in both clusters when the H is moved in z direction.

In a plane perpendicular to the z axis, the potential energy depends on the angle ϕ and the distance ρ. However, the ϕ dependency of the energy surface is weak, as will be shown below. Therefore we assume the energy surface to be independent of ϕ, which provides us with a simple analytical as well as computational tractable model.

Altogether, more than 180 points in the $(z\text{-}\rho)$ plane were calculated. The impurity was moved up to 0.3 Å in the negative (toward Si) z direction, up to 0.6 Å in the positive z direction, and up to 0.75 Å in the ρ direction bisecting two of the threefold mirror planes. The calculated energies for various impurity positions are shown in Fig. 2. The solid lines are fits to Morse potentials.[21]

III. MODEL POTENTIAL

Since the energy for various positions of H parallel to the z axis is well modeled by a Morse potential, an ansatz for a model potential for the whole energy surface was chosen in the form

$$V(z,\rho)=V^M(z,\rho)+\epsilon(\rho), \tag{1}$$

with

$$V^M(z,\rho)=A(\rho)[1-e^{-a(\rho)[z-\tilde{z}(\rho)]}]^2. \tag{2}$$

For fixed ρ, this potential has the form of a Morse potential. The four parameters A, a, $\tilde{z}$, and ϵ vary with ρ, as seen in Fig. 2. For these parameters we assume the following forms:

$$A(\rho)=A_0+A_2\rho^2, \tag{3}$$

$$a(\rho)=a_0+a_2\rho^2, \tag{4}$$

$$\tilde{z}(\rho)=z_0+z_2\rho^2, \tag{5}$$

$$\epsilon(\rho)=\epsilon_0+\epsilon_2\rho^2+\epsilon_4\rho^4. \tag{6}$$

While a quadratic dependence is adequate for the first three parameters, the anharmonicity of the wagging mode enforces the inclusion of a quartic term in the fourth one. These equations completely define our model potential.

The coefficients of Eqs. (3)–(6) are determined in two steps. First, the potential of Eq. (1) is fitted to the energy surface calculated at the *ab initio* level for each ρ, as shown in Fig. 2. In this way, we obtain four ρ-dependent Morse potential parameters A, a, $\tilde{z}$, and ϵ. Second, these four Morse potential parameters are approximated by the functional form of Eqs. (3)–(6). The numerical values of the nine model potential parameters, in atomic units, are in Table I. The energy scale is shifted to be zero at the minimum and z_0 is set to zero.

IV. PERTURBATION APPROACH

Having determined a functional form for the impurity energy surface, the vibrational spectrum can be calculated. We use an analytical perturbative approach. Potential (1) is split into two parts by expanding the Morse part of the potential into a Taylor series around $\rho=0$, and neglecting higher than second-order terms in ρ,

$$V(z,\rho)\simeq V_0(z,\rho)+V_1(z,\rho), \tag{7}$$

TABLE I. The fitted parameters for the model potential in atomic units.

Parameter	ρ^0	ρ^2	ρ^4
A	0.0977	0.0099	
a	0.7502	−0.0997	
$\tilde{z}$	0	−0.1092	
ϵ	0	0.013 54	−0.001 07

TABLE II. The first four eigenvalues and eigenstates for the unperturbed problem. *s* and *w* stand for stretching and wagging, respectively.

Energy	Eigenstate
$E_0=E_0^M+\omega^t$	$\|0\rangle=\|000\rangle$
$E_{1w}=E_0^M+2\omega^t$	$\|1w^+\rangle=\|100\rangle$ $\|1w^-\rangle=\|010\rangle$
$E_{2w}=E_0^M+3\omega^t$	$\|2w^+\rangle=\|110\rangle$ $\|2w\rangle=1/\sqrt{2}(\|200\rangle+\|020\rangle)$ $\|2w^-\rangle=1/\sqrt{2}(\|200\rangle-\|020\rangle)$
$E_{1s}=E_1^M+\omega^t$	$\|1s\rangle=\|001\rangle$

with

$$V_0(z,\rho)=A_0[1-e^{-a_0(z-z_0)}]^2+\epsilon_0+\epsilon_2\rho^2, \tag{8}$$

$$V_1(z,\rho)=V''(z)\rho^2+\epsilon_4\rho^4, \tag{9}$$

where

$$V''(z)=\frac{1}{2}\left.\frac{\partial^2 V^M(z,\rho)}{\partial\rho^2}\right|_{\rho=0}. \tag{10}$$

Potential (8) has the longitudinal and transverse directions decoupled. It consists of a Morse potential in the z direction and a harmonic potential in the ρ direction. The Schrödinger equation can be solved analytically with both these parts. We call $V_0(z,\rho)$ the ''unperturbed potential.''

The coupling between the z and ρ directions is contained in the ''perturbation potential'' $V_1(z,\rho)$ [Eq. (9)]. Note that there is no linear term in ρ, since the first derivative vanishes. The anharmonicity of the wagging mode is also treated in a perturbative manner.

A. Uncoupled spectrum

Since there is no coupling between different directions, the three-dimensional eigenvalue problem decomposes into two one-dimensional Schrödinger equations. Eigenvalues of the three-dimensional problem are written as sums of the one-dimensional eigenvalues, and the corresponding three-dimensional eigenfunctions are products of the one-dimensional eigenfunctions.

The eigenvalues for a particle with mass m in a one-dimensional Morse potential are (see the Appendix)

$$E_n^M=A_0-\frac{a_0^2}{2m}(k-n-1/2)^2, \tag{11}$$

with

$$k=\sqrt{\frac{2mA_0}{a_0^2}}. \tag{12}$$

The eigenvalues for a one-dimensional harmonic potential are

TABLE III. The unperturbed frequencies for hydrogen and deuterium in phosphorus-doped silicon in cm^{-1}.

Transition	H	D
$E_0\rightarrow E_{1w}$	843	596
$E_0\rightarrow E_{2w}$	1686	1192
$E_0\rightarrow E_{1s}$	1631	1168

$$E_n^H=\omega^t(n+1/2), \tag{13}$$

where $n=0,1,...$, and the (transverse) frequency is

$$\omega^t=\sqrt{\frac{2\epsilon_2}{m}}. \tag{14}$$

The lowest four modes of the three-dimensional unperturbed problem are listed in Table II. For the eigenstates, the abbreviation $|n\ m\ l\rangle=\chi_n(x)\chi_m(y)\psi_l(z)$ is used, where χ_n are the eigenstates of a particle in a harmonic potential and ψ_l those in a Morse potential. The explicit expressions for the χ_k and ψ_l functions are in the Appendix.

The spectrum can now be calculated by means of Eqs. (11)–(14), the eigenvalues of Table II and the potential parameters of Table I. Numerical values for hydrogen and deuterium are given in Table III. Note that the frequencies corresponding to $E_0\rightarrow E_{1s}$ would be 1698 cm^{-1} (1201 cm^{-1}) for H (D) if calculated from the curvature of the potential at its minimum. The reduction by 4.0% (2.7%) is due to the anharmonicity inherent to the Morse potential. In Fig. 3 (4) the corresponding spectrum of H (D) vibrations is shown in column I.

Including the zero-point energy[22] of 1684 cm^{-1}, the energy of the second wagging H mode amounts to 3370 cm^{-1}.

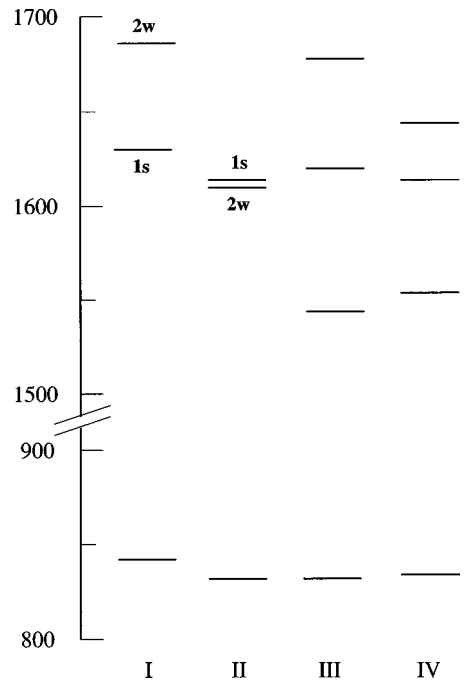

FIG. 3. Spectrum of H vibrational modes in cm^{-1}. Column I: unperturbed (Morse potential along z, harmonic potential along ρ); II: perturbed but uncoupled; III: coupled; IV: experimental values.

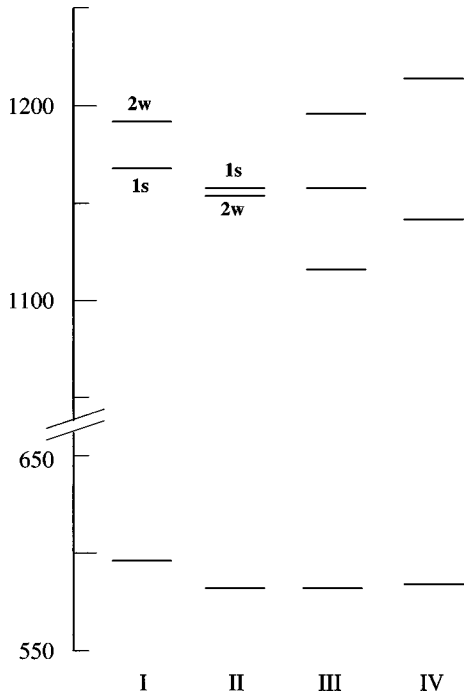

FIG. 4. Spectrum of D vibrational modes. Notations are the same as in Fig. 3.

An inspection of Fig. 2 shows[23] that this energy lies well within the mapped region of the potential energy surface, and is not in the vicinity of any saddle point. The second transverse and first longitudinal modes are nearly degenerate. This leads to the Fermi resonance discussed below.

B. Perturbed spectrum

The coupling between the longitudinal and transversal directions of the potential and terms higher than quadratic in ρ is treated by perturbation theory. We write the full Hamiltonian as

$$\mathrm{H}=\mathrm{H}_0+V''(z)\rho^2+\epsilon_4\rho^4, \tag{15}$$

with the eigenstates and eigenvalues of H_0 in Table II. The matrix elements of H in the basis of the unperturbed eigenstates are listed in Table IV. We use the notation $\sigma_\rho^2=1/\sqrt{2\epsilon_2 m}$, with ϵ_2 the harmonic coefficient of the transverse potential given in Table I. The terms including σ_ρ^2 in the energies of Table IV result from $\langle\chi_k|\rho^n|\chi_l\rangle$ and are easy to calculate. W_{kl} are defined by $W_{kl}=\langle\psi_k|V''|\psi_l\rangle$, where

TABLE IV. Matrix elements of the perturbation calculation. Energies are in cm^{-1}.

Expression	Energy	H	D
$\langle 1s\|\mathrm{H}\|1s\rangle$	$E_{1s}+W_{11}\sigma_\rho^2+\epsilon_4 2\,\sigma_\rho^4$	1614	1159
$\langle 1s\|\mathrm{H}\|2w\rangle$	$-W_{10}\sigma_\rho^2$	65.9	39.9
$\langle 2w\|\mathrm{H}\|2w\rangle$	$E_{2w}+W_{00}3\,\sigma_\rho^2+\epsilon_4 14\,\sigma_\rho^4$	1610	1155
$\langle 2w^{\pm}\|\mathrm{H}\|2w^{\pm}\rangle$	$E_{2w}+W_{00}3\,\sigma_\rho^2+\epsilon_4 12\,\sigma_\rho^4$	1620	1159
$\langle 1w^{\pm}\|\mathrm{H}\|1w^{\pm}\rangle$	$E_{1w}+W_{00}2\sigma_\rho^2+\epsilon_4 6\,\sigma_\rho^4$	815	582
$\langle 0\|\mathrm{H}\|0\rangle$	$E_0+W_{00}\sigma_\rho^2+\epsilon_4 2\,\sigma_\rho^4$	0	0

TABLE V. Theoretical and experimental vibrational frequencies for hydrogen and deuterium in phosphorus-doped silicon in cm^{-1}.

Impurity	Theory	Expt.[a]	Impurity	Theory	Expt.[a]
H	815	809.5	D	582	584.7
	1546	1555.4		1117	1141.5
	1620	1615.5		1159	
	1678	1645.5		1197	1215.5

[a]Reference 8.

$|\psi_k\rangle$ are the eigenstates of the Morse potential. We calculated these one-dimensional integrals numerically.

Only nonzero perturbation terms are shown in Table IV, and it is seen that only $|1s\rangle$ and $|2w\rangle$ are coupled, reducing the evaluation of the perturbed spectrum to a 2×2 matrix eigenvalue problem. However, this is just an approximation. In principle, $|1s\rangle$ and $|2w\rangle$ also couple to the ground state $|0\rangle$. Since the difference between E_{1s} and E_{2w} to E_0 is large, the influence of this coupling on the perturbed eigenstates is small. In fact, an explicit treatment of these coupling terms shows that the vibrational frequencies change by less than 0.5%. Thus we neglect these couplings since they complicate the calculation unnecessarily.

The energy values in the two last columns of Table IV are given relative to $\langle 0|\mathrm{H}|0\rangle$ and the corresponding frequencies are plotted in column II of Figs. 3 and 4. We find a dramatic change relative to the unperturbed frequency for the second wagging mode, which is lowered from 1686 to 1610 cm^{-1}, and becomes even lower than the stretching mode at 1614 cm^{-1}. This demonstrates the importance of including higher than quadratic terms when modeling the energy surface in the transverse direction. Furthermore, since the frequencies of the two states are now almost identical, the coupling between these states becomes very important. This is a typical example of a Fermi resonance, as has been predicted by Zheng and Stavola.[8]

Setting $H_{11}=\langle 1s|\mathrm{H}|1s\rangle$, $H_{12}=\langle 1s|\mathrm{H}|2w\rangle$, and $H_{22}=\langle 2w|\mathrm{H}|2w\rangle$, the eigenvalue problem of the 2×2 perturbation matrix has the solutions[24]

$$E_\pm=\tfrac{1}{2}(H_{11}+H_{22})\pm\tfrac{1}{2}\sqrt{\delta^2+4|H_{12}|^2}, \tag{16}$$

with eigenstates

$$|\varphi_+\rangle=\cos\,\alpha\; e^{-i\phi/2}|1s\rangle+\sin\,\alpha\; e^{i\phi/2}|2w\rangle, \tag{17}$$

$$|\varphi_-\rangle=-\sin\,\alpha\; e^{-i\phi/2}|1s\rangle+\cos\,\alpha\; e^{i\phi/2}|2w\rangle, \tag{18}$$

where $\delta=H_{11}-H_{22}$, $\tan 2\alpha=2|H_{12}|/\delta$, $0\leqslant 2\alpha\leqslant\pi$, and $H_{12}=e^{-i\phi}|H_{12}|$.

For hydrogen, the numerical values for $E_\pm$ are 1678 and 1546 cm^{-1}, respectively. Thus, the energies are essentially shifted by the coupling $|H_{12}|$. A very similar result is found for deuterium. The final calculated vibrational spectra for H and D in P-doped Si as well as the experimental results are listed in Table V and shown in Figs. 3 and 4. A good agreement between theory and experiment is found for all bands, although the motions of all atoms other than H are neglected.

To check the soundness of our analytical perturbative approach, we also calculated the vibrational spectrum numeri-

cally. The energy surface was directly used without any fitting to an analytical form. The vibrational spectrum was then obtained with the help of a numerical solver for the Schrödinger equation. The resulting bands differ by less than 0.7% from our analytical results. Thus our simple method, based on an analytical approximation of the energy surface and the treatment of the coupling terms by perturbation theory, is quite appropriate.

To give a rough estimate of the error introduced by assuming a rotationally invariant energy surface, we scanned the energy surface at z_0 in two directions perpendicular to the z axis, enclosing an angle ϕ of 30° and 60° to our original (z-ρ) plane. The potential slightly increases for increasing ϕ, indicating that our frequencies are slightly underestimated. In order to quantify the effect of the ϕ dependence on the frequencies, Eq. (6) of the model potential was extended to $\epsilon(\rho,\phi)=\epsilon(\rho)+\epsilon_{22}[1-\cos(3\phi)]\rho^2+\epsilon_{42}[1-\cos(3\phi)]\rho^4$ with $\epsilon(\rho)$, as given in Eq. (6). The unknown parameters ϵ_{22} and ϵ_{42} were estimated to be 0.00127 Ha/a_B^2 and 0.00045 Ha/a_B^4, respectively. Note that for an exact determination of the parameters, the whole (z-ρ) energy surface had to be scanned for at least one value of ϕ. The ϕ-dependent part of the potential was then included in the perturbation theory. As expected, an increase of the frequencies resulted, but the change was less than 6% for all the frequencies. Thus we can conclude that a much more demanding analysis including a scan of the whole three-dimensional energy surface would not change the frequencies dramatically.

The square of the corresponding wave functions for H in P-doped Si are shown in Fig. 5. A strong mixing is found for the two coupled states $|1s\rangle$ and $|2w\rangle$. The mixing angle α between the wagging and stretching states is nearly $\pi/4$ for H as well as for D. The wagging and stretching states have almost the same contribution to the coupled states, and it is in fact no longer possible to distinguish between wagging and stretching for the coupled modes. This is also reflected in the ratio of the intensities of the coupled modes. The ratio is given by[8] $I_+/I_-=\cos^2\alpha/\sin^2\alpha$. Our calculated value for H is 1.06 very close to unity. For D, it is 1.11, just a little bit higher than for H. The experimental values[8] are 1.3 for H and 2.5 for D. While a rather good agreement between theory and experiment is found for H, the experimental ratio of intensities for D is about a factor of 2 larger than the calculated value. It is questionable whether this large difference can be explained by our theoretical approach, where differences between H and D do only enter in the kinetic-energy term. However, these intensity ratios are very sensitive to the actual values of the unperturbed levels and to the coupling.

V. CONCLUSIONS

On the basis of a first-principles potential-energy surface, we calculated the vibrational frequencies of hydrogen and deuterium in phosphorus-doped silicon. We showed that the three-dimensional energy surface in the vicinity of the H (D) impurity is well approximated by an analytic expression based on Morse potentials with ρ-dependent parameters. We treated the coupled potential by analytical perturbation theory, and showed that the coupling in the longitudinal and transverse direction is important to understand the entire spectrum. The calculated frequencies are in very good agreement with the experimental results. In particular, theory confirms the recently proposed explanation by Zheng and Stavola for the vibrational bands by means of a Fermi resonance.

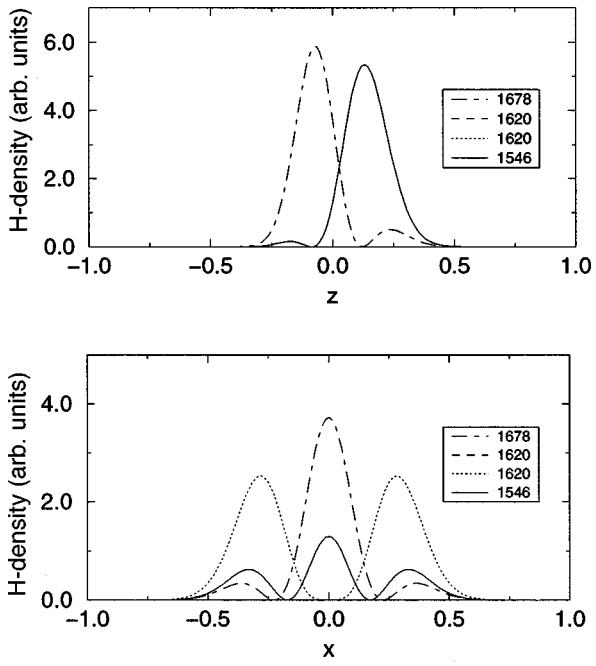

FIG. 5. The eigenstates of H in P-doped Si from perturbation theory. The square of the wave function is shown in the z direction (longitudinal) and in the x direction (transversal) for the frequencies around 1600 cm^{-1}. The strong mixing of the $|1s\rangle$ and the $|2w\rangle$ state is visible in the upper figure. Distances are in Å.

ACKNOWLEDGMENTS

The authors would like to thank H. U. Suter and M. Stavola for enlightening discussions. This work was partially supported by the Swiss National Science Foundation. The services provided by the national supercomputing center CSCS have been essential for this study.

APPENDIX: A PARTICLE IN AN EXTERNAL POTENTIAL

The energies and eigenstates are given for a particle with mass m in an external potential. The Morse potential[21] and the harmonic potential[25] are considered. Atomic units are used.

1. Morse potential

$$\text{Potential: } V(z)=A_0(1-e^{-a_0(z-z_0)})^2,$$

$$\text{Energy: } E_n=A_0-\frac{a_0^2}{2m}(k-n-1/2)^2,$$

$$n=0,1,2,...,$$

$$\text{Functions: } \psi_0(z)=C_0e^{-ky}y^{k-1/2},$$

$$\psi_1(z)=C_1e^{-ky}y^{k-3/2}(ky-k+1),$$

$$k=\sqrt{\frac{2mA_0}{a_0^2}},\quad y=e^{-a_0(z-z_0)}.$$

C_0 and $C_1$are normalization factors.

2. Harmonic potential

Potential: $V(x)=\epsilon_2 x^2$,

Energy: $E_n=\left(n+\frac{1}{2}\right)\omega$,

$n=0,1,2,...,$

Functions: $\chi_0(x)=\left(\frac{c}{\pi}\right)^{1/4}e^{-cx^2/2}$,

$\chi_1(x)=\left(\frac{4c^3}{\pi}\right)^{1/4}x\ e^{-cx^2/2}$,

$\chi_2(x)=\left(\frac{c}{4\pi}\right)^{1/4}(1-2cx^2)e^{-cx^2/2}$,

$\omega=\sqrt{\frac{2\epsilon_2}{m}},\quad c=\sqrt{2m\epsilon_2}$.

*Present address: Department of Physics and Astronomy, University of British Columbia, Vancouver, B.C., Canada V6T 1Z1.

[1] S. J. Pearton, J. W. Corbett, and M. Stavola, *Hydrogen in Crystalline Semiconductors* (Springer-Verlag, Berlin, 1992).
[2] S. K. Estreicher, Mater. Sci. Engr. Rep. **14**, 319 (1995).
[3] N. M. Johnson, C. Herring, and D. J. Chadi, Phys. Rev. Lett. **56**, 769 (1986).
[4] K. Bergman, M. Stavola, S. J. Pearton, and J. Lopata, Phys. Rev. B **37**, 2770 (1988).
[5] L. Korpás, J. W. Corbett, and S. K. Estreicher, Phys. Rev. B **46**, 12 365 (1992).
[6] S. K. Estreicher and R. Jones, Appl. Phys. Lett. **64**, 1670 (1994).
[7] Z. N. Liang, C. Haas, and L. Nielsen, Phys. Rev. Lett. **72**, 1846 (1995).
[8] J.-F. Zheng and M. Stavola, Phys. Rev. Lett. **76**, 1154 (1996).
[9] G. G. DeLeo, W. B. Fowler, T. M. Sudol, and K. J. O'Brien, Phys. Rev. B **41**, 7581 (1990).
[10] S. K. Estreicher, L. Throckmorton, and D. S. Marynick, Phys. Rev. B **39**, 13 241 (1989).
[11] A. Amore Bonapasta, A. Lapiccirella, N. Tomassini, and M. Capizzi, Phys. Rev. B **39**, 12 630 (1989).
[12] S. B. Zhang and D. J. Chadi, Phys. Rev. B **41**, 3882 (1990).
[13] P. J. H. Denteneer, C. G. Van de Walle, and S. T. Pantelides, Phys. Rev. B **41**, 3885 (1990).
[14] A. Amore Bonapasta, P. Giannozzi, and M. Capizzi, Phys. Rev. B **42**, 3175 (1990).
[15] Yu Zhou, R. Luchsinger, and P. F. Meier, Phys. Rev. B **51**, 4166 (1995).
[16] H. U. Suter, N. Paschedag, and P. F. Meier, Philos. Mag. B **72**, 193 (1995).
[17] R. Luchsinger, P. F. Meier, N. Paschedag, H. U. Suter, and Yu Zhou, Philos. Trans. R. Soc. London, Ser. A **350**, 203 (1995).
[18] GAUSSIAN 94, Revision B.3, M. J. Frisch *et al.*, Gaussian, Inc., Pittsburgh, PA, 1995.
[19] S. H. Vosko, L. Wilk, and M. Nusair, Can. J. Phys. **58**, 1200 (1980).
[20] The sophisticated reader knows that 1 eV $\leftrightarrow$ 8065.5 cm^{-1}.
[21] P. M. Morse, Phys. Rev. **34**, 57 (1929); E. U. Condon and P. M. Morse, *Quantum Mechanics* (McGraw-Hill, New York, 1929).
[22] The two wagging modes contribute 843 cm^{-1} to the zero-point energy of H, the stretching mode 841 cm^{-1}.
[23] For $|z|\leqslant 0.4$ Å the potential was calculated up to $\rho=0.75$ Å. These values are not included in Fig. 2.
[24] See, e.g., C. Cohen-Tannoudji, B. Diu, and F. Laloë, *Mécanique Quantique* (Hermann, Paris, 1973).
[25] T. Mayer-Kuckuk, *Atomphysik* (Teubner, Stuttgart, 1985).